COLD SPRING HARBOR
Molecular Case Studies

RESEARCH REPORT

Histological and molecular plasticity of ALK-positive non-small-cell lung cancer under targeted therapy: a case report

Markus Ball,[1,2] Petros Christopoulos,[2,3] Martina Kirchner,[1] Michael Allgäuer,[1] Regine Brandt,[1] Hauke Winter,[2,4] Claus Peter Heußel,[2,5] Felix Herth,[2,6] Stefan Fröhling,[7,8] Rajkumar Savai,[9,10] Mark Kriegsmann,[1,2] Peter Schirmacher,[1,8] Solange Peters,[11] Michael Thomas,[2,3] Albrecht Stenzinger,[1,2] and Daniel Kazdal[1,2]

[1]Institute of Pathology, University Hospital Heidelberg, 69120 Heidelberg, Germany; [2]Translational Lung Research Center (TLRC) Heidelberg, German Center for Lung Research (DZL), 69120 Heidelberg, Germany; [3]Department of Thoracic Oncology, Thoraxklinik at University Hospital Heidelberg, 69120 Heidelberg, Germany; [4]Department of Thoracic Surgery, Thoraxklinik at University Hospital Heidelberg, 69126 Heidelberg, Germany; [5]Diagnostic and Interventional Radiology with Nuclear Medicine, Thoraxklinik at University Hospital Heidelberg, 69120 Heidelberg, Germany; [6]Department of Pulmonology, Thoraxklinik at University Hospital Heidelberg, 69120 Heidelberg, Germany; [7]Department of Translational Medical Oncology, National Center for Tumor Diseases (NCT) Heidelberg and German Cancer Research Center (DKFZ), 69120 Heidelberg, Germany; [8]Center for Personalized Medicine Heidelberg (ZPM), 69120 Heidelberg, Germany; [9]Department of Lung Development and Remodelling, Max Planck Institute for Heart and Lung Research, 61231 Bad Nauheim, Germany; [10]Universities of Giessen and Marburg Lung Center (UGMLC), German Center for Lung Research (DZL), 35392 Gießen, Germany; [11]Oncology Department, Lausanne University Hospital, 1011 Lausanne, Switzerland

Abstract With medical progress in cancer therapy, tyrosine kinase inhibitors (TKIs) became a standard of care for many cancer types. But the broad range of possible targeted therapies was accompanied by a plethora of potential resistance mechanisms, of which many have still to be identified. Here, we present the case of a patient with an *EML4–ALK* translocated non-small-cell lung cancer treated with four different TKIs. Her tumor developed not only a well-known *ALK*–TKI resistance mutation but also underwent a histological transformation from adenocarcinoma to squamous cell carcinoma. To confirm a shared monoclonal origin of the phenotypically different tumors, a phylogenetic reconstruction was conducted: This revealed a cluster of mutations including *NFE2L2*, *KMT2D*, and *MLH1*, which are possible triggering events for the transformation.

[Supplemental material is available for this article.]

Corresponding authors: albrecht.stenzinger@med.uni-heidelberg.de; daniel.kazdal@med.uni-heidelberg.de

Ontology term: lung adenocarcinoma

Published by Cold Spring Harbor Laboratory Press

doi:10.1101/mcs.a006156

INTRODUCTION

Non-small-cell lung cancer (NSCLC) is classified based on the World Health Organization's criteria of light microscopy and immunohistochemistry (IHC). It includes the two main subtypes lung adenocarcinoma (ADC) and squamous cell carcinoma (SqCC). Comprehensive molecular workup in routine molecular diagnostics does not only allow the identification of well-established targetable driver alterations like *EGFR* and *BRAF* mutations or fusions of *ALK*, *ROS1*, *RET*, and *NTRK1/2/3*, but it also can aid in differentiating two independent primary tumors from a primary tumor and a subsequent relapse. *EML4–ALK* translocations

are well-known driver alterations in ADC but rarely reported in SqCCs (Dragnev et al. 2014). Here, we describe the evolution of an *ALK*-positive lung tumor under tyrosine kinase inhibitor (TKI) treatment from an ADC to a SqCC, supporting the suggested alternative resistance mechanism of a recent study (Park et al. 2019).

RESULTS

Case Presentation

We present the case of a histological and genetic transformation to an *EML4–ALK*-positive ADC to a SqCC under therapy over a period of 5 yr (Fig. 1A). A 49-yr-old female patient, ex–light smoker (5 pack years) since 2015, was first diagnosed with an *EML4–ALK* translocated pulmonary ADC in December 2016, based on an endobronchial biopsy of the left main bronchus. Further, initial diagnosis revealed brain metastases, pleural infiltration, and pleural effusion, but no other distant metastases. Rebiopsies following progress were taken in 2019, 2020, and 2021 as computed tomography (CT)-guided pleural biopsies from the fourth posterior intercostal space on the left, the left dorsal side, of a lesion from the fifth to eighth rib on the left side, respectively. The first two biopsies (2016, 2019) were diagnosed consistently as ADC, supported by immunohistochemical expression of TTF-1 and CK7 (Fig. 1B). Apart from single cells the tumor did not show any expression of p63, a marker commonly used to assess squamous differentiation (Supplemental Fig. S1). However, in the two later biopsies, ADC could not be diagnosed, as the tumor cells exhibited clear and solely features of a SqCC with evident keratinization and expression of CK5/6 and p63 but absence of immunoreactivity for TTF-1 and CK7. In all four biopsies tumor cells did not show any PD-L1 expression.

Treatment

First-line treatment started in January 2017 with crizotinib (2 × 250 mg/d). Upon isolated central nervous system (CNS) progression with diffuse brain lesions 2 mo later, whole brain radiotherapy was conducted (10 × 3 Gy). Because of further CNS progression, therapy was switched to alectinib (2 × 600 mg/d) in June 2017, which led to a partial intra- and extracranial remission. In June 2018, stereotactic radiotherapy (6 × 5 Gy) was administered because of oligoprogression in the brain. In April 2019, diffuse tumor growth in the left lung and pleura led to a rebiopsy that revealed the *ALK*:p.I1171N resistance mutation. A switch to brigatinib (180 mg/d) led to stable disease. Disease progression occurred after 15 mo of treatment and triggered another biopsy with a subsequent switch to lorlatinib (100 mg/d) in August 2020. Because of further tumor growth, yet another tissue biopsy was performed in March 2021, and palliative radiotherapy was offered because of infiltration of the spinal canal (thoracic vertebrae 6–9; 12 × 3 Gy). Chemotherapy with carboplatin and pemetrexed was initiated in June 2021 (Fig. 1A) but was poorly tolerated. Therefore, the patient requested cessation of further antineoplastic therapy and opted for best supportive care in July 2021.

Molecular Findings

At the end of 2016, an endobronchial biopsy was taken that tested positive for an *EML4–ALK* translocation (exon 6 NM_019063.5 to exon 20 NM_004304.5) with mutations in *APC*, commonly observed in ADCs, *RANBP2*, and *IRS1* (Fig. 2A). The second biopsy taken in 2019, after relapse under treatment with crizotinib and alectinib, confirmed the initial finding of an *EML4–ALK* translocation and also tested positive for an *ALK*:p.I1171N resistance mutation besides showing additional mutations in *POLE* and *TSC2*.

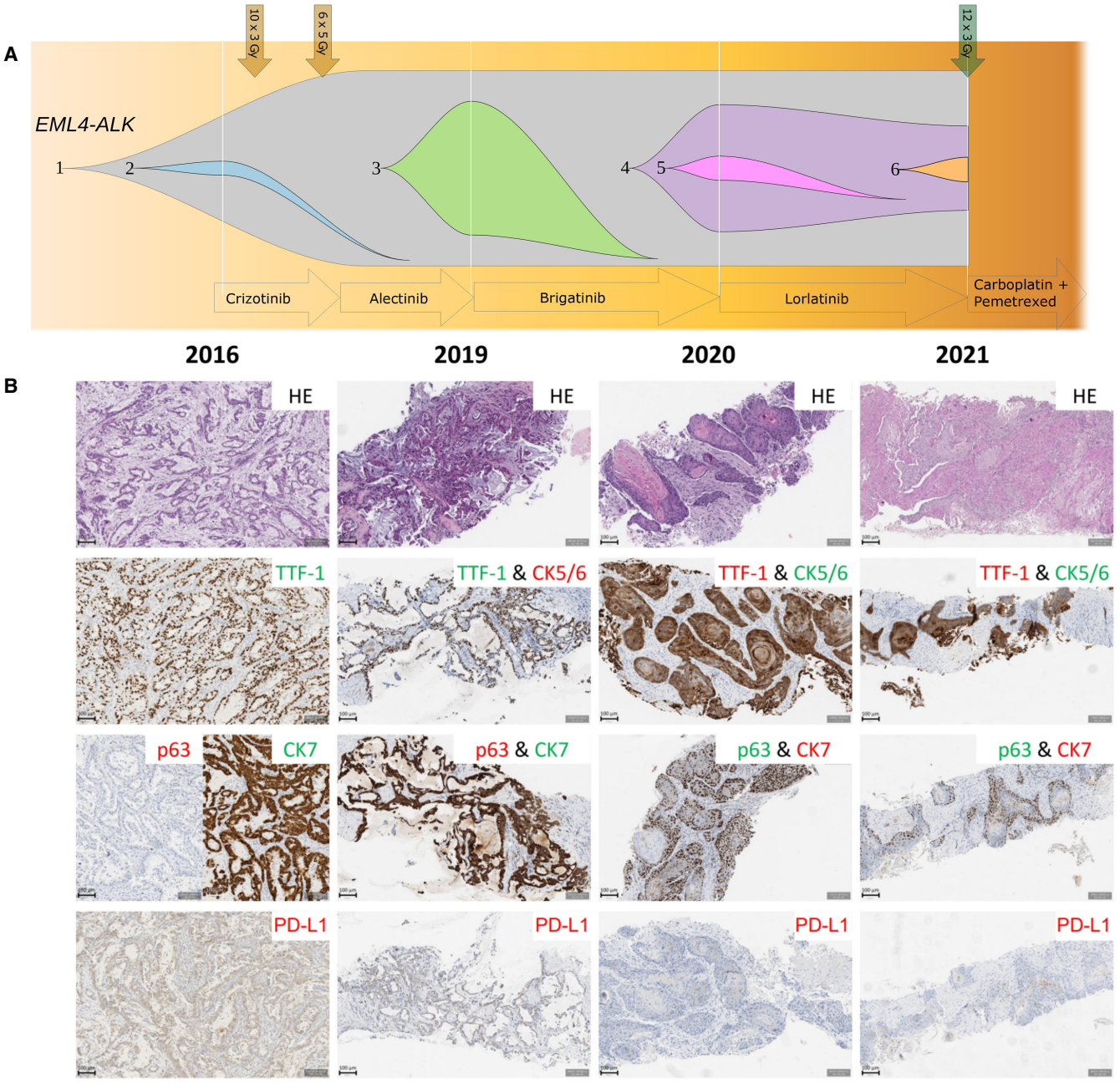

Figure 1. The fishplot (*A*) represents the clonal evolution over time with the development of subclones marked with 1–6. Radiotherapy is indicated by arrows on *top* with fractionation and dosage (in gray). The arrows on *bottom* represent the time and length of treatment, and the white lines indicate the time points biopsies were taken. (*B*) Representative figures of the hematoxylin and eosin (H&E) and immunohistochemical (IHC) stains (either as single or double staining: TTF-1, CK5/6, p63, CK7, PD-L1) demonstrating morphology and protein expression of biopsies taken at the respective time points. Red indicates negativity for the respective marker; green indicates positivity.

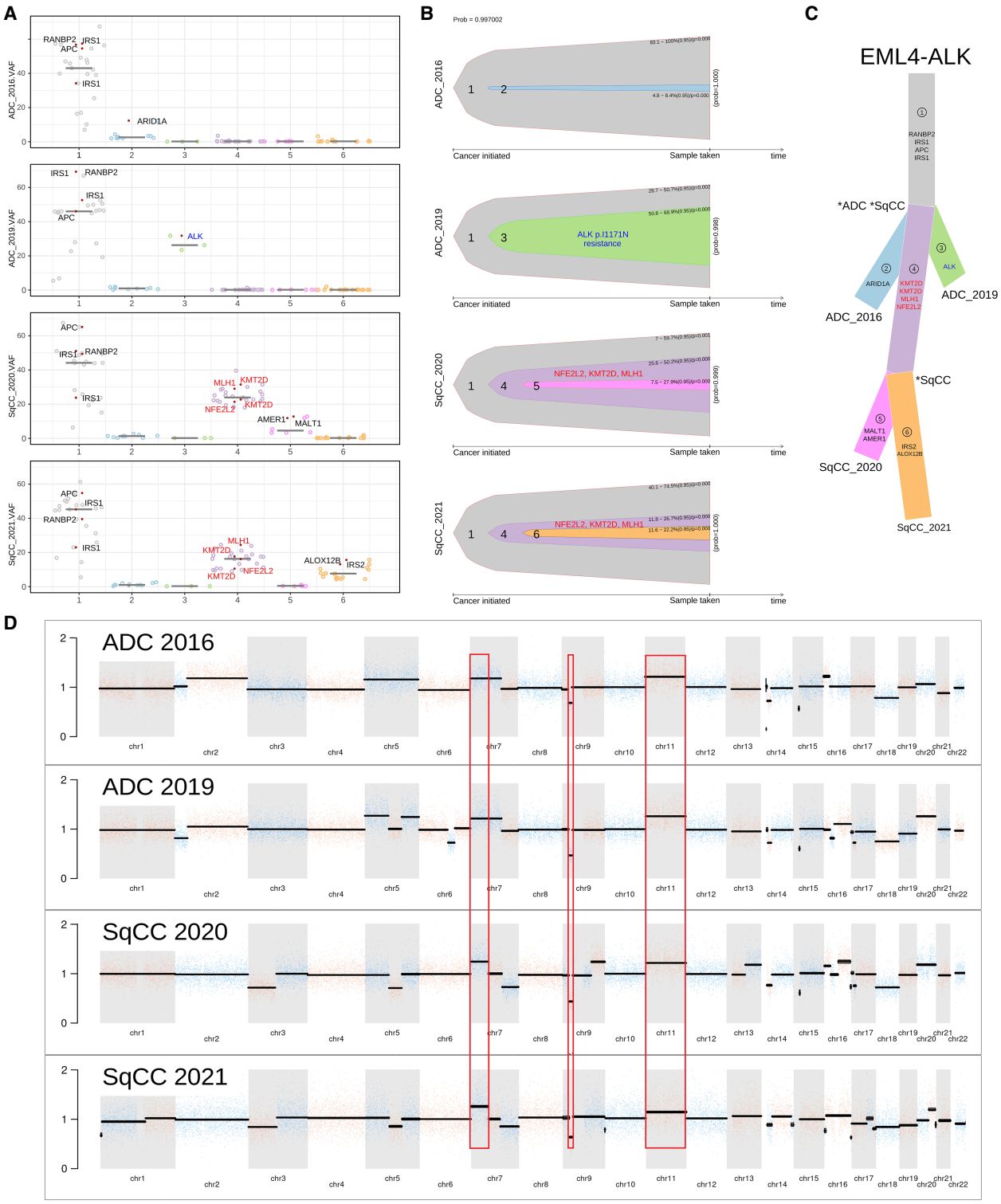

Figure 2. (*A*) The variant allele frequencies (VAFs) of cluster 1–6 for each sample generated with SciClone. Genes defining the respective clusters are shown in the diagram. (*B*) The subclonal architecture for the four biopsies with probabilities from ClonEvol. (*C*) The reconstructed phylogenetic tree with the protein changing mutations defining clones in the branches. The founding clones are marked with an asterisk. (*D*) The genomic regional copy-number variants (CNVs) of the four biopsies are shown. The *y*-axis gives the fold change of the coverage compared to a panel of normals with 1 standing for copy-number-neutral. The black lines with the alternating orange and blue (color change for better visibility) data points represent the mean of called segments. The red highlighted positions indicate early CNV events common for all four samples before diverging.

The biopsies taken in 2020 and 2021 shared a common set of additional mutations along with *MLH1*, *KMT2D*, and *NFE2L2*. The initial *EML4–ALK* translocation and most of the mutations of the initial biopsy were also present, but the 2020 and 2021 biopsies were lacking the resistance mutation detected in 2019.

We performed a phylogenetic reconstruction based on the genetic data generated in the course of clinical routine molecular diagnostics. First, we wanted to confirm that the tumor biopsies were of monoclonal origin. Second, we wanted to explore whether selection of a squamous component in the context of a mixed histology at baseline might have occurred.

To this end, a clonal clustering of single-nucleotide polymorphisms (SNPs) was performed using the R package SciClone, which resulted in six clusters (Fig. 2A,B). The phylogenetic tree (Fig. 2C) includes cluster 1 with alterations in *EML4–ALK*, *APC*, *RANBP2*, *IRS1*, and *ETS1*, which proves to be the common ancestor for all four tumor samples. Cluster 2 is an early subclone of the common ancestor with private mutations in *ARID1A* and *ZFHX3* detected in the 2016 ADC sample only. Cluster 3 represents a second ADC subclone with mutations specific to the 2019 biopsy; it contains the resistance mutation *ALK*:p.I1171N as well as a *TSC2* and a *POLE* mutation. Cluster 4 is the common ancestor of both SqCC with *MLH1*, *NFE2L2*, and two *KMT2D* mutations. The SqCCs sequenced in 2020 (cluster 5) and 2021 (cluster 6) both show a high count of additional private mutations acquired in a relatively short period of time. Both SqCCs showed a much higher tumor mutational burden (TMB) with 16.5 mut/mb in 2020 and 20.6 mut/mb in 2021, compared to the ADC samples from 2016 and 2019 with 2.4 mut/mb and 4.7 mut/mb, respectively.

For monoclonal origin confirmation, a copy-number variation (CNV) analysis of all four samples was performed (Fig. 2D). Results showed that all four samples share genomic alterations, marked in red, that can be attributed to an early common event before further divergence. Further, we found a loss of heterozygosity common in both SqCCs but not present in both ADCs for the entire p arm of Chromosome 3, 5q14.1-q23.2 and 7q22.2-q36.3.

DISCUSSION

At diagnosis, the patient exhibited the *EML4–ALK* fusion, an *APC* and two *IRS1* mutations and received crizotinib followed by alectinib. Although the *EML4–ALK* fusion is significantly more prominent in ADCs, Han et al. (2006) describe that down-regulation of IRS1 is mostly prevalent in SqCCs, indicating genetic features associated with a squamous phenotype in the initial tumor biopsy matching a truncating loss of function *IRS1* mutation in all four samples. The development of a primary resistance mutation *ALK*:p.I1171N under crizotinib and alectinib therapy is well-described in the published literature (Ou et al. 2015). But the ensuing phenotypic switch from an ADC to a SqCC as evident by morphology and IHC is a rare event, which has been described previously in a couple of case reports only (Table 1; Gong et al. 2019; Park et al. 2019; Kaiho et al. 2020; Zhang et al. 2021). Interestingly, the transdifferentiation occurred under targeted ALK–TKI-therapy in those five reported cases, in which the administration of alectinib at some point during treatment was a common aspect. Further the transformation from an ADC to a SqCC was suggested as alternate resistance mechanism by Park et al. (2019), who also found a *MLH1* mutation after SqCC transformation, similar to the presented case here.

The mutations in cluster 4 (*NFE2L2*, *KMT2D*, *MLH1*; Table 2; Supplemental Table S2) are the common feature that differentiates the two later SqCC samples from the two ADC samples. Hence, they might have a causative role in triggering this transformation, although we cannot pinpoint a specific mutation without further functional analysis. The prevalence of *NFE2L2* mutations is significantly higher in SqCCs compared to ADCs (Campbell et al. 2016), and the amino acid change p.E82D is classified as likely oncogenic (OnkoKB). The

Table 1. Overview of previous published ALK-positive adenocarcinoma (ADC) and adenosquamous adenocarcinoma (AD-SqCC) case studies showing similar possible histological transformations

Study	Oncogenic driver	Phenotype	ADC sample	SqCC sample	Treatment
Chaft et al. 2012	*ALK* rearrangement	Synchronous ADC and SqCC lesions indicating AD-SqCC	TTF1+; p63−; CK5/6−	TTF1−; p63+; CK5/6+	Crizotinib
Dragnev et al. 2014	*ALK* rearrangement	AD-SqCC	TTF1+; p63−	TTF1−; p63+; p40+	na
Gong et al. 2019	*EML4–ALK* fusion	ADC to SqCC transformation	TTF1+	TTF1− p40+	Crizotinib; ceritinib; alectinib
Park et al. 2019	*ALK*-rearrangement	ADC to SqCC transformation	TTF1+	p63+	Crizotinib; alectinib
Kaiho et al. 2020	*ALK* rearrangement	ADC to SqCC transformation	TTF1+; p40−	TTF1− p40+	Alectinib; ceritinib
Zhang et al. 2021	*ALK* rearrangement	ADC to SqCC transformation	TTF1+; Napsin A+	TTF-1−; Napsin A−; p40+; p63+	Crizotinib; alectinib; ceritinib
This study	*EML4–ALK* fusion	ADC to SqCC transformation	TTF1+; p63−; CK5/6−; CK7+	TTF1−; p63+; CK5/6+; CK7−	Crizotinib; alectinib; brigatinib; lorlatinib

The second column gives the corresponding driver alteration detected in the respective tumor. Columns 4 and 5 show the results of immunohistochemical (IHC) staining for the ADC or AD-SqCCs sample compared to the SqCC sample. The last column summarizes the TKI treatments the patients have received.

role of *KMT2D* as tumor suppressor and epigenetic regulator could also be an attributing factor given that the presence of truncating mutations in *KMT2D* is much more prevalent in SqCCs (6.4%) than in ADCs (0.7%) (Cerami et al. 2012).As mentioned above a *MLH1* mutation has been reported previously in a similar case (Park et al. 2019). Although loss of function of MLH1 is associated with DNA mismatch repair deficiency, the increased TMB of both SqCC samples compared to the earlier ADCs seems plausible, as the *MLH1 mutation* had the highest allelic fraction within the SqCCs founding cluster 4, followed by a rapid accumulation of further mutations in the later biopsies. Similarly, Gong et al. (2019) described in their report an increased TMB in the transformed SqCC of 15.17 mutations/mb. These molecular changes provide a rationale to adapt therapy, for example, giving immune checkpoint inhibitors. But the patient declined another line of treatment.

Table 2. Variant table

Gene	Chromosome	HGVS DNA reference	HGVS protein reference	Variant type	Predicted effect	dbSNP/ dbVar ID	ClinVar accession	Interpretation
MLH1	Chr 3	c.G109C	p.E37Q	SNV	Nonsynonymous SNV	rs63751012	SCV002058107	Likely pathogenic
KMT2D	Chr 12	c.4379dupC	p.L1461Tfs*30	Indel	Frameshift insertion	na	SCV002058108	Likely pathogenic
KMT2D	Chr 12	c.1940delC	p.P647Hfs*283	Indel	Frameshift deletion	rs770315135	SCV002058109	Pathogenic/ likely pathogenic
NFE2L2	Chr 2	c.A246T	p.E82D	SNV	Nonsynonymous SNV	na	SCV002058110	Likely pathogenic

List of mutations only present in both squamous cell carcinoma (SqCC) samples with possible contribution to the transdifferentiation process from adenocarcinoma (ADC) to SqCC.
(SNV) Single-nucleotide variation.

The losses of heterozygosity found in both SqCCs but not in ADCs show no major prevalence in SqCC corresponding to the TCGA data set. Other prevalent CNVs in SqCC, like the recurrent amplification of the q arm of Chromosome 3, were not eminent, indicating no involvement of CNVs in the transdifferentiation in the presented case.

Despite the well-known subtype of adenosquamous carcinoma (AD-SqCC) of the lung showing traits of ADC and SqCC differentiation, and reports of ALK-translocated AD-SqCC cases, which were initially misclassified as SqCC because of sampling bias (Table 1; Chaft et al. 2012; Dragnev et al. 2014), the case presented here strongly indicates a true phenotype change as a possible resistance mechanism to treatment. The result of the genetic evaluation and the (immuno)histological examination clearly separate the two ADC samples from the later SqCC samples. The minor amount of p63-positive tumor cells in the initial biopsy does not qualify to dismiss the diagnosis of an ADC in favor of an adenosquamous carcinoma. Furthermore, the specificity of p63 for SqCC was described by our group to be imperfect in a study of 1244 NSCLCs, with ∼16% of ADC showing positivity for p63 (Kriegsmann et al. 2019). Rather, the subset of p63-positive cells could indicate a subclone that bears the potential to differentiate toward a SqCC phenotype. Even if AD-SqCC cannot be completely excluded, one would have to assume extreme sampling bias leading to two clear ADC followed by two clear SqCC phenotypes, which is very unlikely. However, the recognition of only one histological component at a time in the biopsy at least suggests that there is a strong plasticity in which phenotype and genotype are variable under therapeutic pressure.

Phenotypic plasticity was described to play several roles in cancer development (Gupta et al. 2019). De-differentiation is a well-known mechanism for cancer progression and metastases. Trans-differentiation as an acquired resistance is an emerging theme, which is not well-understood. The presented case demonstrates such a trans-differentiation from ADC to SqCC with acquired alternative resistance mechanism to TKI therapy.

Furthermore, the diagnostic aspect that the SqCC biopsies do not refer to a second carcinoma but to the known primary tumor that has evolved molecularly and possibly phenotypically is of clinical importance and was only detectable by molecular workup. This also implies that clonality analysis by comprehensive molecular analysis on biopsies, as many patients are not detected until stage IV and complete histological workup via resection material is not possible, could be far more important in routine diagnostics.

Possible limitations of our research include the lack of a sequenced germline sample for a clean removal of germline SNPs, as well as the lack of a control baseline for the CNV analysis, but germline analysis is not routinely conducted because of ethical, legal, and economical constrains as all testing was carried out within clinical routine molecular diagnostics. Furthermore, a higher resolution of CNV detection and phylogenetic reconstruction could have been achieved with a whole-genome sequencing (WGS) approach. To obtain deeper insights into the transformation process, complementary analysis including epigenetics and transcriptomics, for example, would be needed. Possible further research in this area could include manipulating genes from cluster 3 in *EML4–ALK*-positive cell lines to trigger a possible transformation.

Conclusion

We support the transformation from ADC to SqCC as a possible alternative resistance mechanism under ALK–TKI-therapy similar to that shown in previous studies (Gong et al. 2019; Kaiho et al. 2020; Park et al. 2019; Zhang et al. 2021). This case study highlights the benefit of comprehensive molecular testing and reveals the evolutionary connection of the lesions despite their histological differences. Finally, we identified candidate molecular alterations

Competing Interest Statement

All authors have completed the ICMJE uniform disclosure form. P. C. reports grants and personal fees from Novartis, Roche, AstraZeneca, Takeda, and personal fees from Pfizer, Chugai, Boehringer, outside the submitted work. C.P.H. reports grants from Siemens, Pfizer, MeVis, Boehringer Ingelheim, German Center for Lung Research, personal fees from Astellas, AstraZeneca, Basilea, Bayer, Boehringer Ingelheim, Bracco MEDA Pharma, Chiesi, Covidien, Essex, Fresenius, Gilead, Grifols, Intermune, Lilly, MSD, Novartis, Pfizer, Pierre Fabre, Roche, Schering-Plough, Siemens, other from GSK, outside the submitted work; in addition, C.P.H. has a patent Method and Device for Representing the Microstructure of the Lungs, IPC8 Class: AA61B5055FI, PAN: 20080208038 issued. F.H. reports personal fees from Uptake, BTG, Olympus, Pulmonx, outside the submitted work. S.F. has a consulting or advisory board membership with Bayer, Illumina,

Roche; received honoraria from Amgen, Eli Lilly, PharmaMar, Roche; received research funding from AstraZeneca, Pfizer, PharmaMar, Roche; and received travel or accommodation expenses from Amgen, Eli Lilly, Illumina, PharmaMar, Roche. P.S. reports personal fees from BMS, MSD, Incyte, Janssen, Amgen, Novartis, Roche and AstraZeneca outside the submitted work. S.P. has consulting and advisory roles with AbbVie, Amgen, AstraZeneca, Bayer, BeiGene, Biocartis, Boehringer Ingelheim, Bristol-Myers Squibb, Clovis, Daiichi Sankyo, Debio-pharm, Eli Lilly, F. Hoffmann-La Roche, Foundation Medicine, Illumina, Incyte, Janssen, Medscape, Merck Sharp and Dohme, Merck Serono, Merrimack, Novartis, Pharma Mar, Phosphoplatin Therapeutics, Pfizer, Regeneron, Sanofi, Seattle Genetics, and Takeda. S.P. has spoken in the following companies' organized public events: AstraZeneca, Boehringer Ingelheim, Bristol-Myers Squibb, Eli Lilly, F. Hoffmann-La Roche, Illumina, Medscape, Merck Sharp and Dohme, Novartis, Pfizer, Prime, Sanofi, and Takeda. S.P. is also the recipient of the following grants and/or research supports: (Sub)investigator in trials (institutional financial support for clinical trials) sponsored by Amgen, AstraZeneca, Biodesix, Boehringer Ingelheim, Bristol-Myers Squibb, Clovis, F. Hoffmann-La Roche, GSK, Illumina, Lilly, Merck Sharp and Dohme, Merck Serono, Mirati, Novartis, Pfizer, and Phoshoplatin Therapeutics. A.S. reports grants and personal fees from Bayer, BMS; grants from Chugai and personal fees from Astra Zeneca, MSD, Takeda, Seattle Genetics, Novartis, Illumina, Thermo Fisher, Eli Lilly, Takeda, outside the submitted work. D.K. reports personal fees from AstraZeneca, Bristol-Myers Squibb, Pfizer, Lilly, Agilent and Takeda outside the submitted work. The remaining authors declare no conflict of interest.

Received October 19, 2021; accepted in revised form December 22, 2021.

that could have been causative for this rare event; thus, this case study may give rise to further in-depth investigations.

METHODS

Immunohistochemical staining of thyroid transcription factor 1 (TTF-1), CK7, CK5/6, p63, and PD-L1 (see Supplemental Table S1 for antibody details) were conducted using an autostainer (BenchMark ULTRA, Ventana Medical Systems) according to the manufacturer's instructions. PD-L1 positivity was defined as linear membranous PD-L1 staining in ≥1% of tumor cells.

DNA was extracted automatically from six 10-µm FFPE sections of each sample by applying a Maxwell 16 FFPE Tissue LEV DNA Purification Kit on a Maxwell 16 Research system (both Promega). DNA concentrations were determined with the Qubit HS DNA assay (Thermo Fisher Scientific) according to the manufacturers' protocols.

A TruSight Oncology 500 panel (Illumina) was used for targeted DNA sequencing according to the manufacturers protocol and as previously described (Kazdal et al. 2019). Mutation and CNV calling was completed by GATK 4.2. Only "PASS" mutations not present in gnomAD with a frequency of >0.1% and an allelic fraction of >2% in at least one sample were used for phylogenetic reconstruction. Fusion detection was performed either using a custom-designed (Pfarr et al. 2016) targeted RNA-seq panel (AmpliSeq technology, Thermo Fisher Scientific) or by using the anchored multiplex polymerase chain reaction (PCR)-based FusionPlex Lung kit (Archer DX) according to the manufacturer's protocol.

For clustering, phylogenetic reconstruction, and plotting we used the R packages SciClone (Miller et al. 2014), ClonEvol (Dang et al. 2017), and fishplot (Miller et al. 2016), respectively.

ADDITIONAL INFORMATION

Data Deposition and Access

Mutations in Table 2 have been deposited in ClinVar (https://www.ncbi.nlm.nih.gov/clinvar/) with the accession numbers SCV002058107–SCV002058110.

Ethics Statement

The authors are accountable for all aspects of the work in ensuring that questions related to the accuracy or integrity of any part of the work are appropriately investigated and resolved. Tissues were used in accordance with the ethics committee of Heidelberg University (S-145/2017).

Author Contributions

P.C., A.S., and D.K. conceptualized the report; M.B., P.C., M.A., M.Ki, and R.B. established the methodology; M.B. was responsible for the software; M.B. and D.K. performed the validation; M.B., A.S., and D.K. performed the formal analysis; M.Ki., P.C., and D.K. performed the investigation; P.S. and A.S. provided the resources; M.Kr., R.B., and D.K. curated the data; M.B., M.A., P.C., M.T., A.S., and D.K. wrote the original draft; H.W., C.P.H., F.H., S.F., R.S., M.Kr., S.P., P.S., and A.S. performed the writing review and edited; Visualization, M.B. and D.K. performed the visualization; A.S. and D.K. supervised; and P.S. and A.S. administered the project.

REFERENCES

Campbell JD, Alexandrov A, Kim J, Wala J, Berger AH, Pedamallu CS, Shukla SA, Guo G, Brooks AN, Murray BA, et al. 2016. Distinct patterns of somatic genome alterations in lung adenocarcinomas and squamous cell carcinomas. *Nat Genet* **48:** 607–616. doi:10.1038/ng.3564

Cerami E, Gao J, Dogrusoz U, Gross BE, Sumer SO, Aksoy BA, Jacobsen A, Byrne CJ, Heuer ML, Larsson E, et al. 2012. The cBio cancer genomics portal: an open platform for exploring multidimensional cancer genomics data. *Cancer Discov* **2:** 401–404. doi:10.1158/2159-8290.CD-12-0095

Chaft JE, Rekhtman N, Ladanyi M, Riely GJ. 2012. *ALK*-rearranged lung cancer adenosquamous lung cancer masquerading as pure squamous carcinoma. *J Thorac Oncol* **7:** 768–769. doi:10.1097/JTO.0b013e31824c9485

Dang HX, White BS, Foltz SM, Miller CA, Luo J, Fields RC, Maher CA. 2017. ClonEvol: clonal ordering and visualization in cancer sequencing. *Ann Oncol* **28:** 3076–3082. doi:10.1093/annonc/mdx517

Dragnev KH, Gehr G, Memoli VA, Tafe LJ. 2014. *ALK*-rearranged adenosquamous lung cancer presenting as squamous cell carcinoma: a potential challenge to histologic type triaging of NSCLC biopsies for molecular studies. *Clin Lung Cancer* **15:** e37–e40. doi:10.1016/j.cllc.2014.01.003

Gong J, Gregg JP, Ma W, Yoneda K, Moore EH, Daly ME, Zhang Y, Williams MJ, Li T. 2019. Squamous cell transformation of primary lung adenocarcinoma in a patient with *EML4-ALK* fusion variant 5 refractory to ALK inhibitors. *J Natl Compr Canc Netw* **17:** 297–301. doi:10.6004/jnccn.2019.7291

Gupta PB, Pastushenko I, Skibinski A, Blanpain C, Kuperwasser C. 2019. Phenotypic plasticity: driver of cancer initiation, progression, and therapy resistance. *Cell Stem Cell* **24:** 65–78. doi:10.1016/j.stem.2018.11.011

Han C, Cho J, Moon J, Kim H, Kim S, Shin D, Chang J, Ahn C, Kim S, Chang Y. 2006. Clinical significance of insulin receptor substrate-I down-regulation in non-small cell lung cancer. *Oncol Rep* **16:** 1205–1210. doi:10.3892/or.16.6.1205

Kaiho T, Nakajima T, Iwasawa S, Yonemori Y, Yoshino I. 2020. ALK rearrangement adenocarcinoma with histological transformation to squamous cell carcinoma resistant to alectinib and ceritinib. *Onco Targets Ther* **13:** 1557–1560. doi:10.2147/OTT.S236706

Kazdal D, Endris V, Allgauer M, Kriegsmann M, Leichsenring J, Volckmar AL, Harms A, Kirchner M, Kriegsmann K, Neumann O, et al. 2019. Spatial and temporal heterogeneity of panel-based tumor mutational burden in pulmonary adenocarcinoma: separating biology from technical artifacts. *J Thorac Oncol* **14:** 1935–1947. doi:10.1016/j.jtho.2019.07.006

Kriegsmann K, Cremer M, Zgorzelski C, Harms A, Muley T, Winter H, Kazdal D, Warth A, Kriegsmann M. 2019. Agreement of CK5/6, p40, and p63 immunoreactivity in non–small cell lung cancer. *Pathology* **51:** 240–245. doi:10.1016/j.pathol.2018.11.009

Miller CA, White BS, Dees ND, Griffith M, Welch JS, Griffith OL, Vij R, Tomasson MH, Graubert TA, Walter MJ, et al. 2014. SciClone: inferring clonal architecture and tracking the spatial and temporal patterns of tumor evolution. *PLoS Comput Biol* **10:** e1003665. doi:10.1371/journal.pcbi.1003665

Miller CA, McMichael J, Dang HX, Maher CA, Ding L, Ley TJ, Mardis ER, Wilson RK. 2016. Visualizing tumor evolution with the fishplot package for R. *BMC Genomics* **17:** 880. doi:10.1186/s12864-016-3195-z

Ou SH, Greenbowe J, Khan ZU, Azada MC, Ross JS, Stevens PJ, Ali SM, Miller VA, Gitlitz B. 2015. I1171 missense mutation (particularly I1171N) is a common resistance mutation in *ALK*-positive NSCLC patients who have progressive disease while on alectinib and is sensitive to ceritinib. *Lung Cancer* **88:** 231–234. doi:10.1016/j.lungcan.2015.02.005

Park S, Han J, Sun JM. 2019. Histologic transformation of *ALK*-rearranged adenocarcinoma to squamous cell carcinoma after treatment with *ALK* inhibitor. *Lung Cancer* **127:** 66–68. doi:10.1016/j.lungcan.2018.11.027

Pfarr N, Stenzinger A, Penzel R, Warth A, Dienemann H, Schirmacher P, Weichert W, Endris V. 2016. High-throughput diagnostic profiling of clinically actionable gene fusions in lung cancer. *Genes Chromosomes Cancer* **55:** 30–44. doi:10.1002/gcc.22297

Zhang Y, Qin YP, Xu HG, Yao QH, Gao YL, Feng YS, Ren JL. 2021. Case report: a case report of a histological transformation of *ALK*-rearranged adenocarcinoma with high expression of PD-L1 to squamous cell carcinoma after treatment with alectinib. *Pathol Oncol Res* **27:** 637745. doi:10.3389/pore.2021.637745